Asian Journal of Chemistry; Vol. 35, No. 10 (2023), 2336-2348

ASIAN JOURNAL OF CHEMISTRY

https://doi.org/10.14233/ajchem.2023.28051

Synthesis, Characterization, DNA Synergy and Molecular Docking Studies of Novel 1,10-Phenanthroline Derived Mixed Ligand Metal(II) Complexes

S. Syed Ali Fathima[1,*] and M. Mohamed Sahul Meeran[2]

[1]International Research Centre, Department of Chemistry, Kalasalingam Academy of Research and Education, Krishnankoil-626126, India
[2]SGS Gulf Limited-Jafza, Dubai, United Arab Emirates

*Corresponding author: E-mail: syed.s@klu.ac.in

Received: 29 May 2023; *Accepted*: 23 June 2023; *Published online*: 28 September 2023; AJC-21381

The effect of tumour and all its related costs, both human and commercial factor is driving the exploration for novel curative medicines. Although platinum-based anticancer drugs have shown considerable success, their use is complicated by a number of drawbacks. Therefore, this study is mainly designed for transition metal complex based chemotherapeutic agents to reduce the obstacles for platinum-based anticancer agents presently used. Herein, novel mixed ligand-metal(II) complexes derived from 9-anthraldehyde, 2-aminophenol, metal chlorides and 1,10-phenanthroline (co-ligand) were synthesized and characterized using several spectral techniques, which revealed that they possess an octahedral structure. The interaction of calf thymus DNA (CT-DNA) with synthesized compounds confirmed that the compounds are binded with DNA *via* intercalation. The mode of interaction was affirmed by the docking simulations, where the synthesized compounds were docked with EGFR protein and 1B-DNA through intercalation. The biological screening results revealed that the synthesized complexes exhibited superior anti-pathogenic screening properties compared to ligands. The proliferation resistance against cancer cells and free radical scavenger studies of prepared compounds indicated that the presence of heterocyclic ligand is an important factor for boosting the anticancer potential and radical scavenger skill.

Keywords: Transition metal complex, Octahedral geometry, DNA synergy, Anticancer potential.

INTRODUCTION

Schiff bases and their metal complexes form a variety of clinical compounds with the amazing potential of biological activities including anticancer, anticonvulsant and antioxidant [1]. Numerous studies suggest that a large number of cancer tissues, such as breast and brain cancer cells, carry more copper than regular cells. Although the most effective platinum-based compounds for treating various tumours, these compounds (*e.g.* cisplatin) are still controlled by dose-dependent side effects, hereditary and drug disorders [2,3]. These shortcomings have enabled scientists to identify alternative chemotherapy strategies based on transition metals with useful clinical features [4-7].

Copper(II) is ubiquitously found in all biological systems, where it serves as both a catalyst and a structural cofactor. Consequently, it plays a pivotal role in redox chemistry and several metabolic reactions [8]. Also, it is an important part of angiogenesis such as tumour growth, invasion and metastasis [9-11]. Hence, copper-based metal complexes to be substituted for platinum-based agents in the modern scenario as probable antitumor medicines [6,12,13].

The field of clinical chemistry has experienced an upsurge in recent years due to the implementation of multiple coordinating ligands. Such compounds have shown effective in distinguishing and regulating the impacts of metal ions within the biological systems [14]. Mixed ligand complexes, also known as ternary compounds, have the ability to serve as a synthetic technique for modifying the biological characteristics of metal complexes. Furthermore, 1,10-phenanthroline derived ternary compounds have been extensively used in DNA studies and in many fields, including bioinorganic and medicinal sciences [15].

The biological action of Schiff bases increases upon chelation and some drugs when administered as metal chelates increased the antitumour activity and inhibit the unwanted cell multiplication. Hence, this work deals with the synthesis, characterization and biological evaluation of novel mixed ligand complexes

of metal chlorides derived from 9-anthraldehyde, 2-aminophenol and 1,10-phenanthroline (co-ligand). The findings demonstrate potential in the development and implementation of innovative and valuable DNA probes for antibacterial, antioxidant and anticancer purposes.

EXPERIMENTAL

The chemicals used in this work were of AnalaR grade and can be used without additional purification. 9-Anthraldehyde, 2-aminophenol, 1,10-phenanthroline, calf-thymus DNA, PBR322 DNA were purchased from Sigma-Aldrich, USA. All the analytical solvents were obtained from Merck chemicals, USA.

The elemental analysis was carried out in Perkin-Elmer-240 elemental analyzer. The molar conductivity of the complexes in DMSO (10^{-3} M) solution was measured at room temperature using deep vision 601 model digital conductivity meter. The vibration spectral data have been derived by using FT-IR Shimadzu model IR-Affinity-1 spectrophotometer using KBr discs. Electronic spectra have been derived using Shimadzu UV Vis-1800 spectrometer at room temperature. ^{1}H & ^{13}C NMR spectral data of zinc complexes are recorded by using Bruker 400MHz Advance III HD Nanobay NMR spectrometer with DMSO-d_6 as a deuterated solvent. The mass spectral analysis were performed by using JEOL-AccuTOF JMS-T100LC mass spectrometer equipped with a custom-made electrospray interface (ESI). The X-band of the EPR spectrum was recorded by JES-FA 200 spectrometer at liquid nitrogen temperature (77 K) and at room temperature (300 K). EDAX spectral data of the complexes are performed by AMETEK-EDAX (Analyzer). The SEM and colour mapping images are retrieved from the instrument model ZE ISS EVO 18 Research. The powder XRD was taken using Shimatzu XRD-6000 X-ray diffractometer with 2θ ranges from 10-80º and the surface morphology was studied by a field emission scanning electron microscopy (FESEM) (Model SUPRA 40) with a voltage of 30 KV. The absorption spectra are recorded using UV-visible spectrophotometer (Shimadzu model UV-1601) at room temperature for DNA binding studies.

Synthesis of Schiff base ligand (L): An ethanolic solution of 2-aminophenol (0.4062 g, 2 mmol) was added to 9-anthraldehyde (0.2091 g, 2 mmol) dissolved in 50 mL of ethanol in a 1:1 molar ratio. The mixture was sonicated and then refluxed for 5 h. A dark yellow precipitate was obtained, the precipitate was washed with dry ethanol (**Scheme-I**).

Ligand (HL): Yield: 86%; *m.w.*: 297; colour: dark yellow; Anal. calcd. (found) % for $C_{21}H_{15}NO$: C, 85.91 (83.34); H, 4.37, (4.33); N, 4.83 (4.44%); λ_{max}, cm^{-1} in DMSO 38910 ($\pi\rightarrow\pi^*$); 27624, $n\rightarrow\pi^*$; FT-IR (ν_{max}, cm^{-1}): 1665 (-CH=N); ^{1}H NMR (DMSO-d_6) (δ): (aromatic) 6.74-7.97 (m), (-CH=N) 9.14 (s), (-OH) 9.40; ^{13}C NMR (DMSO-d_6) (δ): (aromatic) 115.85-146.97, (-CH=N) 152.38, C-OH 158.07; ESI-MS: 298 *m/z*.

Synthesis of mixed ligand complexes [ML_2(phen)]: An ethanolic solution of metal(II) salt (M = Cu^{2+}, Co^{2+}, Ni^{2+} and Zn^{2+}) was added to a mixture of 0.5874 g (2 mmol) of Schiff base ligand (HL) dissolved in 50 mL of ethanol and 0.1982 g (1 mmol) of 1,10-phenanthroline dissolved in 20 mL of ethanol with a molar ratio of 1:2:1. The final mixture was sonicated and then refluxed for 8 h. Then, the obtained crystalline precipitate was washed with ethanol, filtered and dried in oven at 37 ºC (**Scheme-II**). The crude product was recrystallized from methanol:ethanol (1:1) mixture.

[CuL_2(phen)]: Yield: 85%; *m.w.*: 836; colour: brown; Anal. calcd. (found) % for $[CuC_{54}H_{36}N_4O_2]$: C, 77.54 (77.43); H, 4.34 (4.31); N, 6.70 (6.60); Cu, 7.60 (7.50); $\Lambda_m \times 10^{-3}$ (Ω^{-1} mol^{-1} cm^{-2}): 12; μ_{eff} (B.M.): 1.85; λ_{max}, cm^{-1} in DMSO 15290 (*d-d*); FT-IR: 1676 ν(-CH=N);1275 ν(C-O); 545 ν(M-O), 446 ν(M-N); ESI-MS: 836 *m/z*.

[CoL_2(phen)]: Yield: 84%; *m.w.:* 831; colour: dark brown; Anal. calcd. (found) % for $[CoC_{54}H_{36}N_4O_2]$: C, 77.99 (77.21); H, 4.36 (4.31); N, 6.74 (6.72); Co, 7.08 (7.05); $\Lambda_m \times 10^{-3}$ (Ω^{-1} mol^{-1} cm^{-2}): 14; μ_{eff} (B.M.): 4.25; λ_{max} cm^{-1} in DMSO 15037 (*d-d*); FT-IR (KBr disc, cm^{-1}): 1687 ν(-CH=N), 1273 ν(C-O); 551 (M-O), 455 (M-N); ESI-MS: 832.125 *m/z*.

[NiL_2(phen)]: Yield: 79%; *m.w.*: 831; colour: black; Anal. calcd. (found) % for $[NiC_{54}H_{36}N_4O_2]$: C, 77.99 (77.22); H, 4.36 (4.32); N, 6.74 (6.71); Ni, 7.06 (7.03); $\Lambda_m \times 10^{-3}$ (Ω^{-1} mol^{-1} cm^{-2}): 15; μ_{eff} (B.M.): 3.27; λ_{max} cm^{-1} in DMSO 16255 (*d-d*); FT-IR (KBr disc cm^{-1}): 1682 ν(-CH=N), 1266 ν(C-O); 551 ν(M-O), 444 ν(M-N); ESI-MS: 831.221 *m/z*.

[ZnL_2(phen)]: Yield: 89%; *m.w.*: 838; Colour: dirty white; Anal. calcd. (found) % for $[ZnC_{54}H_{36}N_4O_2]$: C, 77.37 (76.32); H, 4.33 (4.23); N, 6.68 (6.35); Zn, 7.80 (7.55); $\Lambda_m \times 10^{-3}$ (Ω^{-1} mol^{-1} cm^{-2}) 17; μ_{eff} diamagnetic; FT-IR (KBr disc, cm^{-1}): 1688 ν(-CH=N); 1274 ν(C-O); 555 ν(M-O), 457 ν(M-N); ^{1}H NMR (DMSO-d_6) (δ): (aromatic) 7.11-8.67 (m), 8.86 (s); ^{13}C NMR (DMSO-d_6) (δ): (aromatic) 115.45-144.19, 151.00, 164.01; ESI-MS: 838.456 *m/z*.

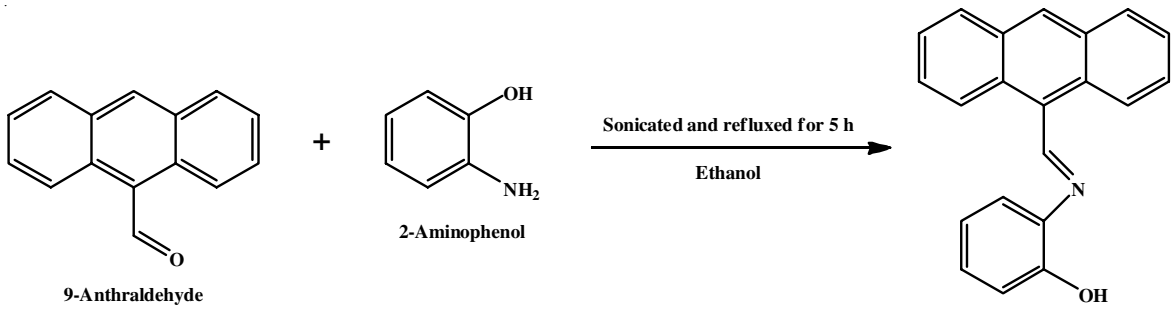

Scheme-I: Synthesis of Schiff base ligand

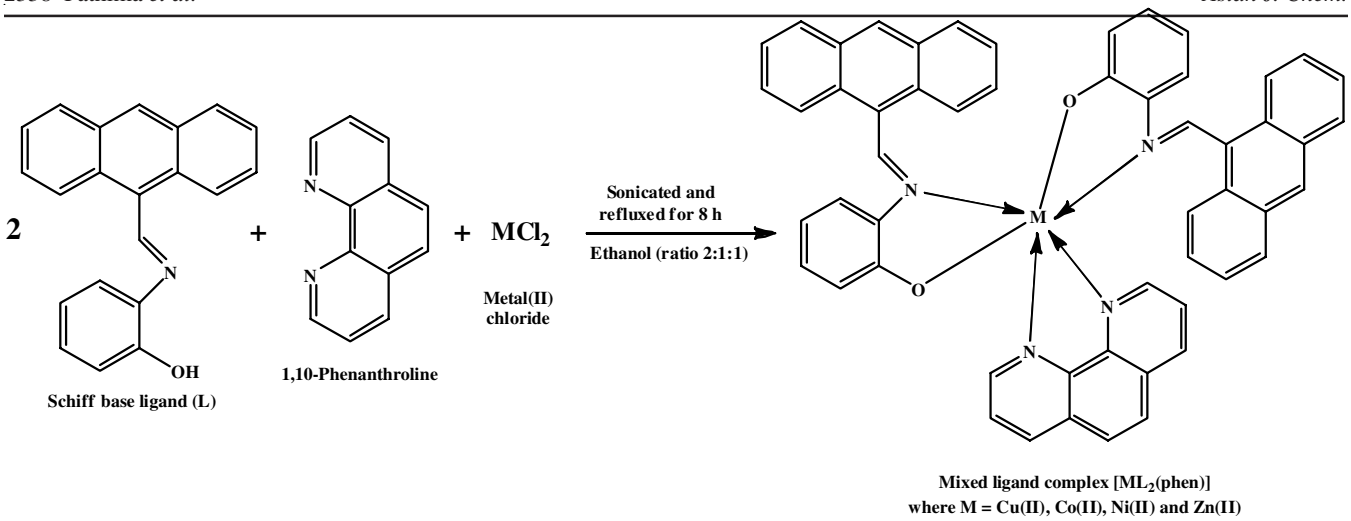

Scheme-II: Synthesis of mixed ligand complexes [ML_2(phen)]

DNA binding experiments: The interaction between complexes and CT-DNA were carried out in Tris-HCl buffer 5 mM Tris-HCl/50 mM NaCl medium (pH 7.2) containing 5% DMSO at room temperature. The absorption spectra were recorded on a Shimadzu model UV-1601 spectrophotometer using cuvettes having 1 cm path length. The concentrated stock solution of synthesized compounds (10^{-3} M) were diluted suitable with a corresponding buffer solution at required concentrations for all the experiments and the spectra of these complexes were recorded before and after the addition of DNA [16]. The interaction of the compound with DNA was obtained from absorption data. These absorption spectral titrations are performed by the incremental addition of nucleic acid to the constant concentration of the complexes. This titration process was repeated until there is no change in the absorption values suggesting the binding saturation [17].

Viscosity measurements: Viscosity measurements of the metal(II) complexes were carried out by Ostwald viscometer at a constant temperature of 30.0 ± 0.1 ºC by using thermostat waterbath. An approximately 0.5 mmol sample of CT-DNA was prepared by sonication to minimize the complexities arising from CT-DNA flexibility [18]. Flow time was measured for all the comp-lexes in thrice using the digital stopwatch and an average flow time was calculated. The data were calculated against η/η_o and the concentration of synthesized compounds, where η is indicated as the viscosity of CT-DNA with metal complexes and η_o is indicated as a viscosity of CT-DNA without metal comp-lexes. Viscosity value of the complexes were measured after calculating the flow time of buffer alone (t_o) using the following formula [19]:

$$\eta = \frac{t - t_o}{t_o}$$

DNA damage studies: The extent of pBR 322 DNA cleavage was monitored by agarose gel electrophoresis in the presence of an activator H_2O_2 as an oxidizing agent [20]. In this reaction super coiled pBR322 plasmid DNA Form I (1 µg) in DMSO (1%, 2 µL) was treated with synthesized compounds (250 µg) and oxidizing agent H_2O_2 (40 mmol, 5 µL). The samples were incubated at 1 h at 310 K. A loading of buffer containing bromophenol blue (0.25%), glycerol (30%) and xylene cyanol (0.25%) was added to a platform fixed with a comb to form slots. The electrophoresis was performed at 50 V for 1 h in TBE (tris-boric acid-EDTA) buffer using 1% agarose gel containing 0.5 µg/mL ethidium bromide. The effectiveness of the synthesized compound was measured by determining the capability of the complexes converting the supercoiled form of DNA to circular form and finally linear form. It was visualized by UV light to photograph the bands [21].

Antimicrobial assay: The MIC value of the synthesized ligand and its metal complexes were tested against bacterial strains (*Staphylococcus aureus*, *Bacillus subtilis* (Gram-positive), *Escherichia coli*, *Klebsiella pneumoniae*, *Salmonella typhi* (Gram-negative) and the fungal strains *viz*. *Aspergillus niger*, *Fusarium solani*, *Curvularia lunata*, *rhizoctonia bataticola*, *Candida albicans*) through a broth dilutions method with the standard antibacterial ampicillin and nystatin, respectively. These test concentration synthesized compounds were preformed from 0.01 to 2.5 mg/mL in the sterile walls of microtiter plates and using 50 µL of sterile nutrient broth. The MIC values are determined by reading each well at 492 nm in an automated micro plate reader [22].

Cytotoxic activity (MTT assay): The *in vitro* cytotoxicity of the synthesized compound on a pair of cancer cell lines such as human breast adenocarcinoma (MCF-7), Human Liver Cancer cell (Hep G2) and non-cancerous cell lines such as HBL-100, established from human breast milk were purchased from National Centre for Cell Science (NCCS) Pune, India by MTT assay. The cell lines are grown in Dulbecco's modified eagles medium (DMEM) (Himedia, India) containing 10% fetal bovine serum (FBS) and 1% antibiotic-antimycotic solutions of all the compounds are prepared in cell culture grade DMSO (Himedia). The effect of treatment of compounds on cell viability was determined using tetrazolium dye by MTT assay. The cytotoxic effect of synthesized compounds against different cell lines was evaluated by MTT assay. Briefly, the cells are seeded in a 96-well plate and kept in CO for attachment and growth for 24 h and then the cells were treated with various

concentrations of complexes dissolved in DMSO and incubated for 24 h. After incubation, the culture medium was removed and 15 mL of the MTT was discarded and DMSO (100 mL/well) was added to dissolve the purple formazan product [23]. The experiment was carried out in triplicates and the medium without compounds served as control. The absorbance was measured calorimetrically at 570 nm using an ELISA microplate reader. The percentage of cell viability was calculated using the following formula:

$$IC_{50} = \frac{\text{OD value of treated cells}}{\text{OD value of untreated cells (control)}} \times 100$$

A graph was plotted with the percentage of cell inhibition versus concentration. From this graph IC_{50} (concentration of compound to kill 50% of the cells) value was calculated.

Hoechst 33258 staining method (Apoptosis): Hoechst 33258 blue fluorescent dye is permeable and binds to DNA in live and dead cells, which is mainly used to detect the different characteristic features of apoptosis process. The generated complexes trigger nuclear alterations and the formation of apoptotic bodies, as evidenced by the application of the Hoechst 33258 staining technique. To analyze the morphological apoptotic changes, 1×10^5 concentration of MCF-7 cancer cells were treated with synthesized complexes for 48 h in a 96-well culture plate. After incubation (48 h), the cells were washed in PBS (phosphate-buffered saline) and stained for 10 min at room temperature in PBS containing *p*-formaldehyde (40%) and Hoechst 33258 (10 mg/mL). The cancer cells for Hoechst staining were grown on sterilized cover slips. After washing once with phosphate buffered saline cells were fixed with 3.7% of formaldehyde in PBS for 10 min, washed once with PBS, stained with 0.4 mg/mL of Hoechst in PBS for 15 min and again washed two times with PBS. Then the cells were observed and imaged by a fluorescence microscope (Olympus, Tokyo, Japan, magnification 20 X) with excitation at 350 nm and emission at 550 nm.

Antioxidant assay: The radical scavenging activity of the synthesized compounds was determined by using DPPH assay. Vitamin C (10 mg/mL DMSO) served as a standard against which the decrease in DPPH solution absorption caused by the addition of an antioxidant could be calculated. In brief, the reagent DPPH (0.1 mM) solution was prepared by dissolving 4 mg of DPPH in 100 mL of ethanol. The different volumes (1-40 µg/mL) of ligand and its metal(II) complexes were made up to 40 µg/mL with DMSO and then 2.96 mL DPPH (0.1 mmol) solution was added. After 20 min incubation at room temperature in dark containing 3 mL of DPPH as control, the absorbance of the reaction mixture was measured at 517 nm. The percentage of radical scavenging activity of the synthesized compounds were calculated using the following formula:

$$\text{Radical scavenging activity (\%)} = \frac{A_{control} - A_{sample}}{A_{control}} \times 100$$

where RSA is the radical scavenging activity; Abs. control is the absorbance of DPPH radical+ ethanol; Abs. sample is the absorbance of DPPH radical and synthesized compounds [24].

Molecular docking: The enzyme EGFR is responsible for the inflammation of the protein data bank. In DNA docking study (PDB ID 1B-DNA) was used to analyze the binding mode of the complexes. To establish the optimized binding modes of the synthesized compounds against DNA and FGFS protein. It was accomplished using AutodockVina software and bilateral molecular graphics program for studying the optimized docking mode between EGFS and the synthesized compounds [25]. The structure of the synthesized compounds is transformed into PDB file format using pymol software.The structure was optimized before docking.

RESULTS AND DISCUSSION

Based on the results of the elemental analysis, it can be observed that the ternary compounds exhibit stoichiometric ratios of 2:1:1 (ligand:metal:co-ligand). Schiff base is soluble in ethanol, but the ternary compounds were soluble in organic solvents like DMF and DMSO. From low conductance values, the synthesized metal(II) complexes are non-electrolytic in nature.

FT-IR studies: The FTIR spectrum of the Schiff base ligand exhibited a band at 1665 cm^{-1} ascribed to (-CH=N) group [26]. In metal(II) complexes, the azomethine groups shifted to 1695-1675 cm^{-1}, which indicate the chelation of -CH=N group to the metal centre. In free ligand, the broad band at 3445 cm^{-1} appeared, which denoted the phenolic (-OH) group in amino phenol moiety. But in the metal(II) complexes, the band corresponds to hydroxyl group was disappeared, which signifies the deprotonation of (-OH) group. The medium peak appeared around 1280-1265 cm^{-1}, which ascribed the phenolic (C-O) group in the complexes owing to the deprotonation of -OH group [27]. The characteristic (-C-O) peak signifies the chelation of this group with metal ion [28]. Two new bands appeared in the low region around 460-440 cm^{-1} and 560-530 cm^{-1}, which are allocated for (M-N) and (M-O) vibrations, respectively, supporting the participation of CH=N group of ligand and heterocyclic nitrogen of co-ligand and O-atom of the aminophenol moiety in ligand with metal(II) ion upon coordination.

Electronic studies and magnetic properties: The UV spectrum of free ligand displays two characteristic peaks in the region of 38910 cm^{-1} and 27624 cm^{-1} owing to $\pi \rightarrow \pi^*$ and $n \rightarrow \pi^*$ transitions, respectively. A small elevation seen at these frequencies may be associated with chelation of free Schiff base ligand. Copper(II) complex produces a broad band in the region 15290 cm^{-1} owing to *d-d* transition ($^2E_g \rightarrow {}^2T_2g$) of Cu(II) ion. This transition band strongly supports the octahedral geometry. The magnetic moment value of Cu(II) 1.85 B.M., which confirms the monomeric nature of the metal ion [29,30]. Similarly, $[CoL_2(phen)]$ complex shows band in the region 15,037 cm^{-1}, which is allocated to transition $^4T_1g \rightarrow {}^4T_2g$ attributed to the octahedral geometry and supported by its magnetic moment value 4.25 B.M. [31].

$[NiL_2(phen)]$ complex exhibits a *d-d* band at 16255 cm^{-1}, which is assigned to the transition attributed to the octahedral geometry and it is also supported by its magnetic moment value of 3.27 B.M. However, Zn(II) complex does not display the *d-d* band owing to its d^{10} electronic configuration and has the

zero magnetic moment [32]. The empirical formula and other spectral outcomes highly supported octahedral geometry. The electronic spectra of Schiff base ligand, copper, cobalt and nickel complexes are shown in Fig. 1.

^{1}H NMR studies: The proton NMR spectrum of the Schiff base ligand exhibited a multiplet around 6.77-7.07 ppm, which is assigned for the aromatic multiplet in the benzene rings and 7.42-8.51 ppm attributed to aromatic protons multiplet in the anthracene moiety. In Schiff base ligand, the peak attributed to the azomethine and hydroxyl group appeared at 9.14 ppm and 9.40 ppm, respectively [33].

In Zn(II) complex, aromatic multiplet for anthracene moiety around 7.55-8.67 ppm and 7.12-7.44 ppm for benzene moiety. The participation of quinoline moiety seems to be around 7.55-8.37 ppm. The proton associated with the -CH=N functional group exhibits a chemical shift deviation of upto 8.86 ppm and -OH proton is completely missing which indicate that the coordination *via* imine and -C-O group to the metal centre.

^{13}C NMR studies: In Schiff base ligand, the carbon environment of phenyl group around 122.77-146.97 ppm for anthracene group and 127.52-131.74 ppm for benzene group. The azomethine group (-CH=N) appears at 152.38 ppm and C-OH peak at 158.07 ppm for the free ligand.

In Zn(II) complex, the azomethine peak was relocated to 164.01 ppm and the characteristic (-C-OH) peak went disappeared owing to the conversion of (-C-O) group at 151.00 ppm designated the coordination of (-CH=N) group and carbonyl group chelated with Zn metal [34]. The carbon environment of the aromatic group around 123.16-141.10 ppm for anthracene group and 126.97-128.07 ppm for benzene group. The involvement of quinoline moiety in chelation appears about 122.16-144.19 ppm. Furthermore, no major modifications in all other signals in Zn(II) complex are appeared.

Mass spectral studies: The molecular ion peak appeared at *m/z* = 297.121 equivalent to the molecular weight of the Schiff base ligand containing the formula [$C_{21}H_{15}NO$]. The fragmented peaks observed for Schiff base ligand at *m/z* 281.361, 219.111, 204.091, 178.081, 128.061 and 78.012 from the fragments of [$C_{21}H_{15}N]^+$, [$C_{16}H_{13}N]^+$, [$C_{16}H_{12}]^+$, [$C_{14}H_{10}]^+$, [$C_{10}H_8]^+$ and [$C_6H_8]^+$, respectively.

The mass fragmentation for copper(II), cobalt(II), nickel(II) and zinc(II) complexes produce the molecular ion peaks at *m/z* 836.210, 832.125 831.221, 838.456, respectively. Copper(II) complex displays a peak at 836.210 correlated to [$C_{54}H_{36}CuN_4O_2]^+$ species equivalent to the molecular weight copper(II) complex. The molecular ion peak observed at *m/z* 297.121

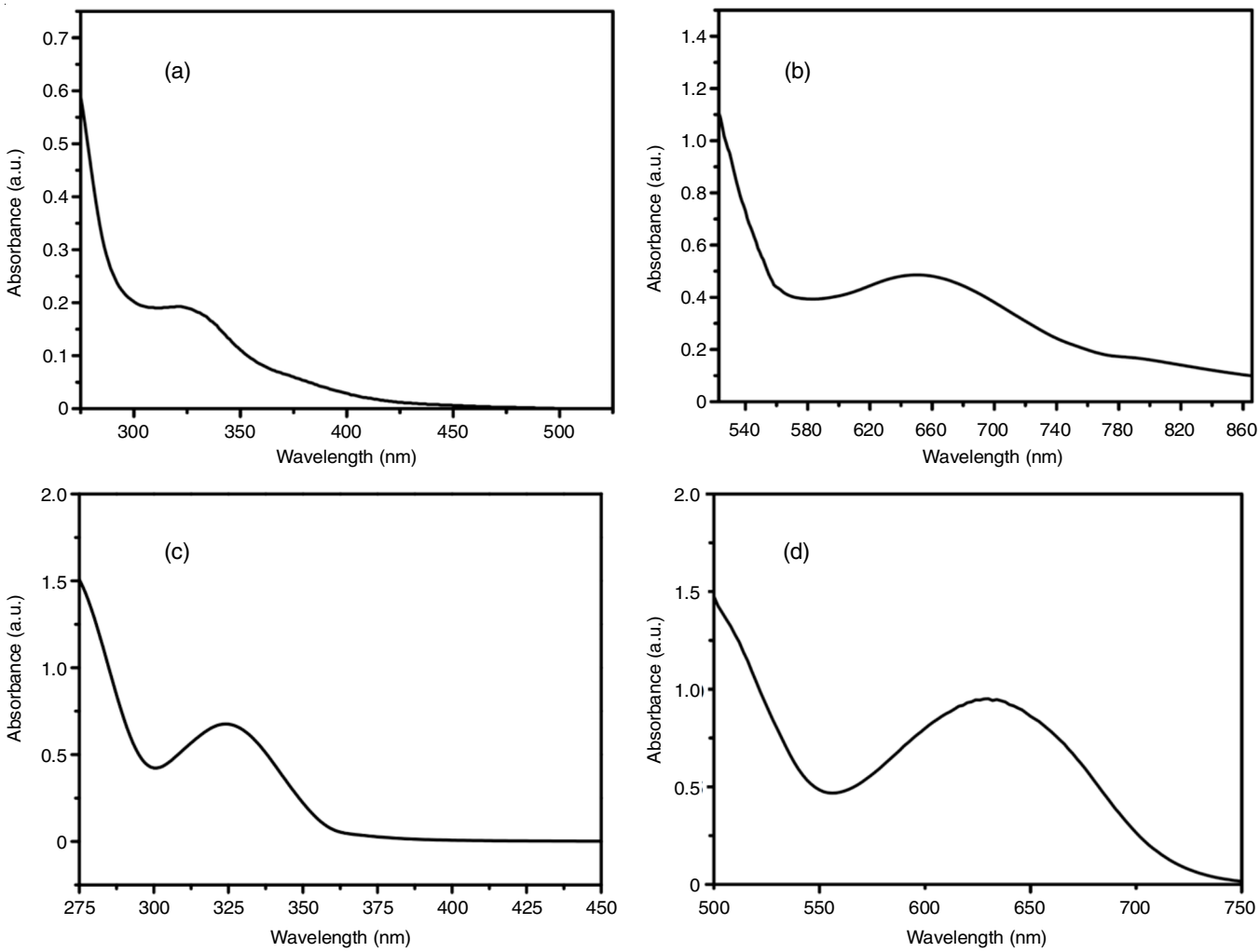

Fig. 1. Electronic spectra of Schiff base ligand (a), [CuL_2(phen)] (b), [CoL_2(phen)] (c) and [NiL_2(phen)] (d) complexes

accredited to [$C_{21}H_{15}NO$], which is equivalent to the molecular weight of Schiff base ligand. The fragmented peaks indicate that the metal complexes belong to the type of [ML_2(phen)], which closely resembles other spectral results.

EPR studies: EPR spectra offer excellent techniques for studying the metal ion environment, molecular geometry and the extent of covalency in the metal-ligand (M-L) interaction [35]. The X band characteristics of this spectrum of [CuL_2(phen)] complex and the spin Hamiltonian parameters of the complex was calculated and it is found that $A_{\parallel}$ (162) > $A_{\perp}$ (67) and $g_{\parallel}$ (2.33) > $g_{\perp}$ (2.08) > g_e (2.0023)] (Table-1). In current study, the value of $g_{\parallel}/A_{\parallel}$ is 143 typically specifies that copper(II) complex has octahedral geometry with the slight distortion [36].

From the g factor values, the geometrical parameter of G, signifying the exchange interactions between the Cu(II) centres in a polycrystalline compound and can be verified by the following formula:

$$G = \frac{g_{\parallel} - 2}{g_{\perp} - 2}$$

If the G value was larger than 4, the tetrahedral axis was aligned in parallel or slightly misaligned and if the G value was smaller than 4, there are significant interactions between the two metals. In this research, the [CuL_2(phen)] compound displays a geometric parameter value of 4.1, which denotes that the [CuL_2(phen)] has no contact (metal-metal contact) exists at Cu(II) centres [37,38]. EPR spectra of [CuL_2(phen)] at room temperature and LNT are laid out in Fig. 2.

SEM images and EDX studies: The SEM images of CuL_2(phen)], [CoL_2(phen)], [NiL_2(phen)] and [ZnL_2(phen)] complexes (Fig. 3) show flakes, spherical, brick, plate and rod fashioned morphologies, respectively. The average particle size 61 nm for Schiff base and 82, 84, 75 and 65 nm for copper, cobalt, nickel and zinc complexes, respectively.

The colour mapping photos provide evidence supporting the presence of components such as carbon (C), nitrogen (N), oxygen (O) and metals in the synthesized compounds. This finding is consistent with the predicted structures. The EDAX spectra and colour mapping image of the synthesized ligand and its metal complexes are shown in Fig. 4.

Biological evaluations

DNA interaction studies: Ultraviolet spectroscopy can furnish important information on the binding mechanism between CT-DNA and the synthesized metal(II) complexes. The absorption peak may change to longer (bathochromism) or shorter (hypochromism) wavelengths, signifying changes in the structure of the DNA. Binding with DNA through intercalation usually creates a stacking interaction between the aromatic chromophore and the base pair of DNA. The degree of hypochromism correlates with the strength of the intercalation. A compound binding to DNA through intercalation usually results in hypochromism and bathochromism, due to the intercalation mode involving a strong π–π* stacking interaction between an aromatic chromophore and the base pairs of DNA [39].

When the metal complex interacts with DNA, it changes in the three-dimensional structure of DNA, resulting in localized bending and separation. Such deformations may inhibit or block cellular processes such as DNA replication and transcription. The introduction of DNA into the complexes results in significant hypochromism ranging from 10% to 25% (Table-2), due to the capability of the complexes to disturb the double-stranded DNA. Compounds are inserted between the base pairs

TABLE-1
THE SPIN HAMILTONIAN PARAMETERS OF Cu(II) COMPLEX IN DMSO SOLUTION AT LIQUID NITROGEN TEMPERATURE (LNT)

Complex	g-tensor			$A \times 10^{-4}$ (cm^{-1})			G
	$g_{\parallel}$	$g_{\perp}$	g_{iso}	$A_{\parallel}$	$A_{\perp}$	A_{iso}	
Cu(II)	2.33	2.08	2.19	162	67	89	4.1

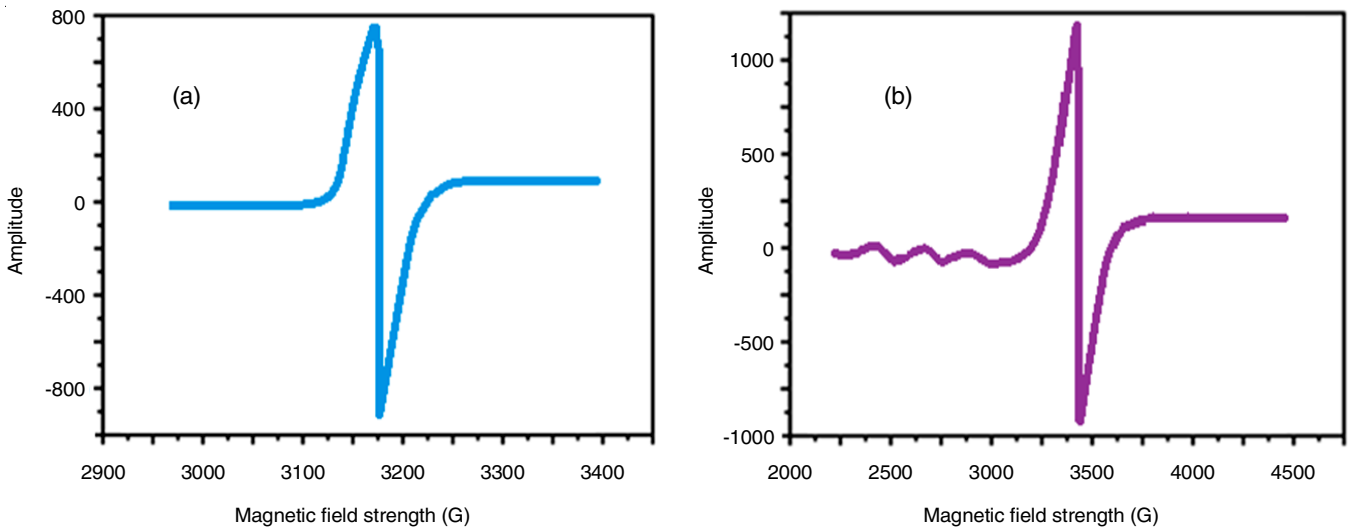

Fig. 2. EPR spectra of [CuL_2(phen)] complex at room temperature (a) and at liquid nitrogen temperature (b)

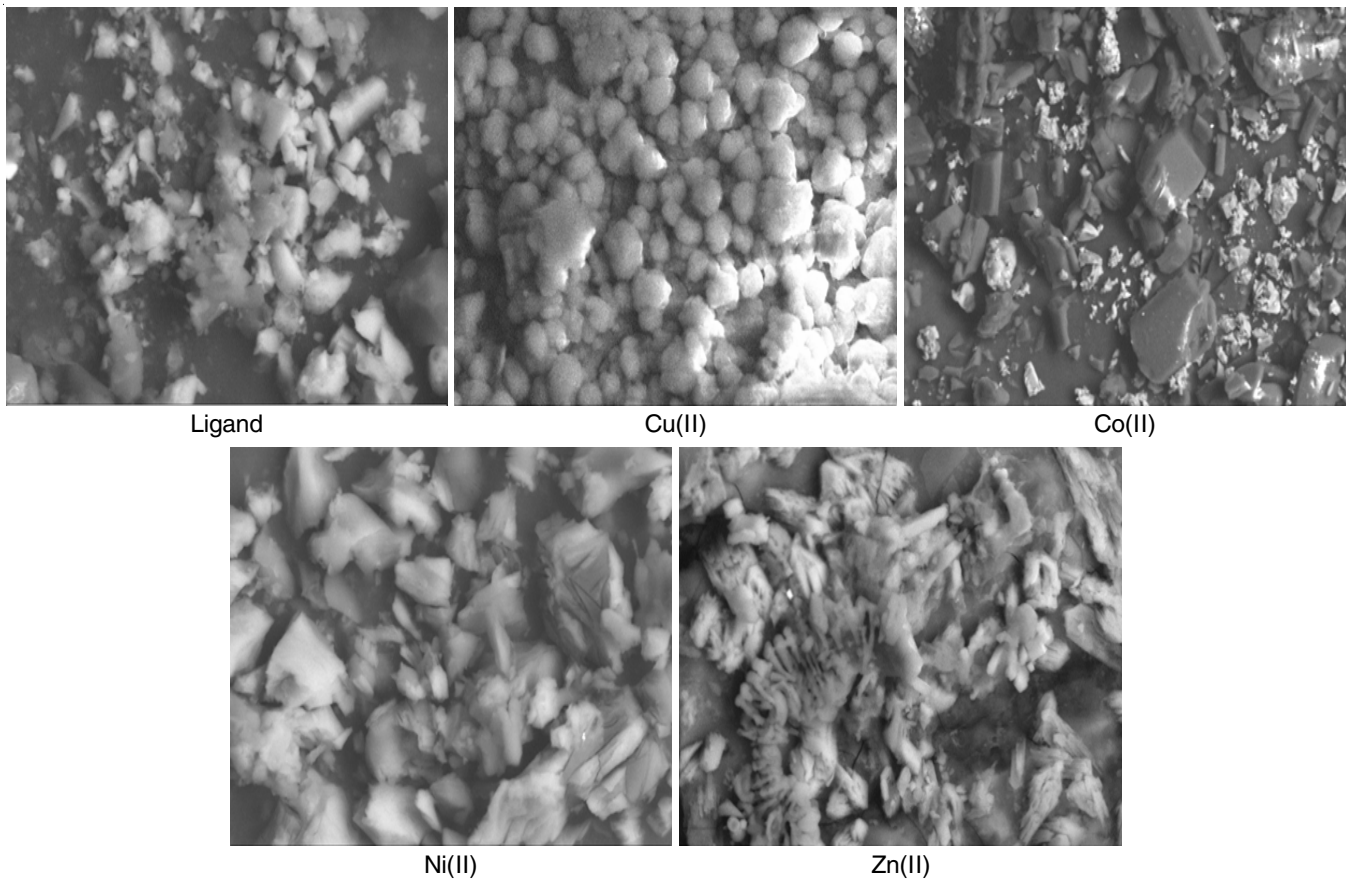

Fig. 3. SEM images of the synthesized ligand and its metal(II) complexes

TABLE-2
ELECTRONIC ABSORPTION PARAMETERS FOR THE INTERACTION OF DNA WITH SYNTHESIZED COMPOUNDS

Complex	λ_{max}		Δλ (nm)	[a]H%	K_b (M^{-1})
	Free	Bound			
Ligand	313	316	3	12.5	3.7×10^4
Cu(II)	323	328	5	24.5	6.8×10^5
Co(II)	315	319	4	23.5	6.4×10^5
Ni(II)	319	322	3	20.3	6.2×10^5
Zn(II)	316	318	2	19.6	5.9×10^5

of nucleotides cause a red shift with a slight change in the wavelength from the original frequency in the region of 310-330 nm due to the π–π* transition of the aromatic group. It inhibits the proliferation of cancer cells and promotes apoptosis. It is widely accepted that alterations to DNA structure caused by intercalator insertion significantly impact biological potential. Generally, the binding of complexes with DNA leads to hypochromism and red shift due to sturdy affinity between the aromatic groups and the base-pairs of nucleic acid [40-42].

The binding constant value (k_b) inferred that the Schiff base displays a weaker affection towards DNA, but metal complexes have a greater affinity. Among the synthesized complexes, [CuL_2(phen)] has greater binding potential value *i.e.* (6.8×10^5 M^{-1}), which is due to small size, ionic radius, positive charge of the metal(II) complexes and heterocyclic co-ligand (1,10-phenanthroline) allows for the improved solubility, selective cellular uptake *via* active transport and high DNA affinity [43]. Therefore, the above strategy signified that ternary compounds interconnected with nucleic acid *via* intercalated mode. The DNA binding study of Cu(II),Co(II) and Ni(II) complexes are shown in Fig. 5.

Hydrodynamic analysis: In classical intercalation, the bond between the base pairs of CT-DNA and synthesized compound enhanced the length of the DNA strand leading to an amplify the viscosity of the DNA. It is well-known that DNA helix twists or bends when intercalation is incomplete, which shortens the helix and increases its viscosity. Whereas, non-intercalated bonding, such as electrostatic or groove binding has little effect [44,45]. Therefore, the results validated that all the synthesized metal(II) complexes can be intercalated with nucleotide, which leads to an increase in the viscosity values (Fig. 6).

Pharmacological evaluation

Antimicrobial activity: In this work, the antimicrobial action of the synthesized Schiff base ligand and its mixed ligands metal(II) complexes was screened against diverse microbes by broth microdilution technique [46]. Ampicillin and nystatin served as the standards for the antibacterial and antifungal activity, respectively. The antibacterial and antifungal activities of all compounds are enlisted in Tables 3 and 4, respectively. Among the synthesized mixed ligand metal(II) complexes, the antibacterial activity studies shows that Cu(II) complex has MIC value from $6.1\text{-}7.0 \times 10^4$ μM and standard drug ampicillin

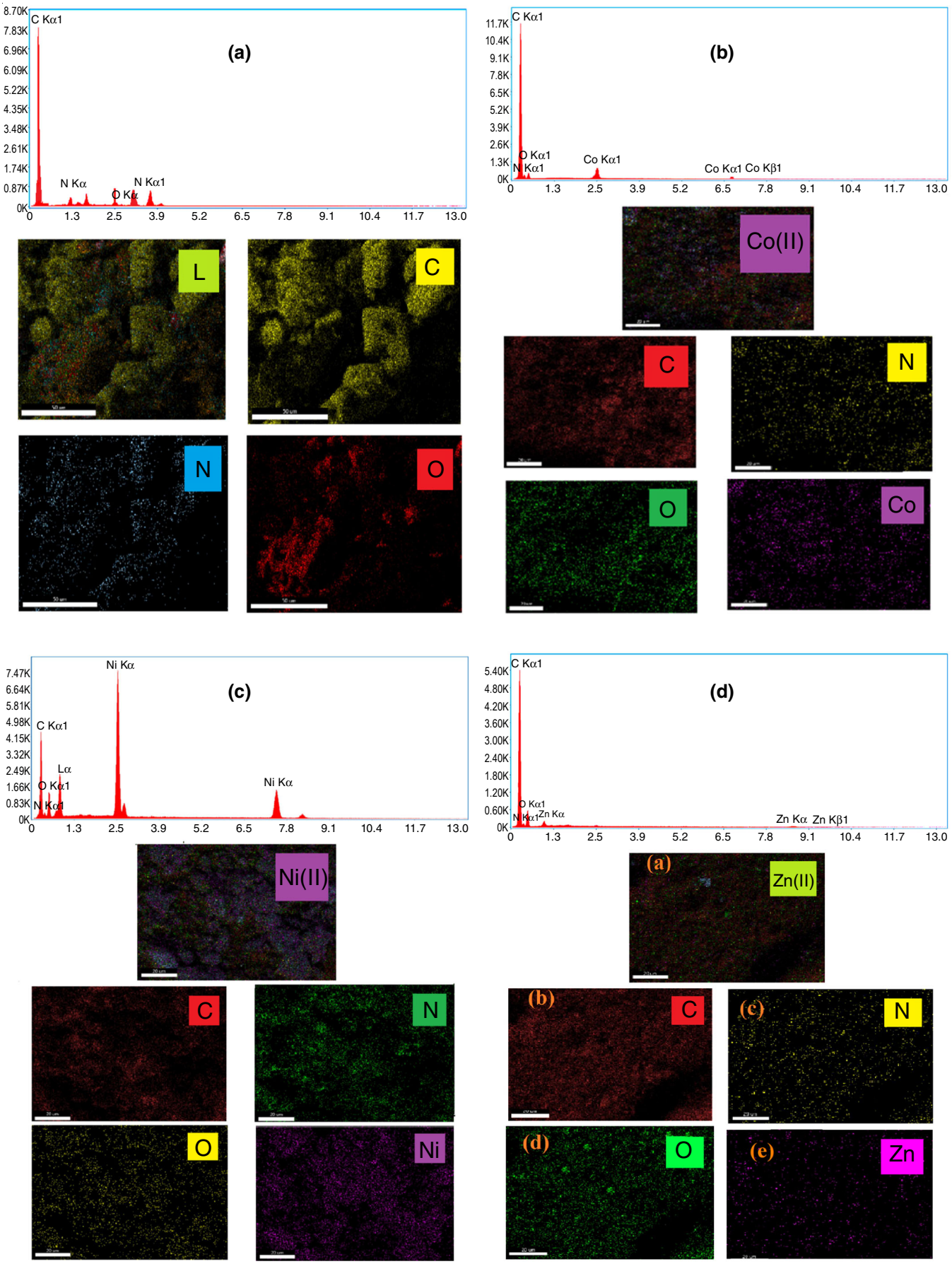

Fig. 4. Elemental colour mapping images of synthesized ligand and its metal(II) complexes possesses elements carbon, nitrogen and oxygen

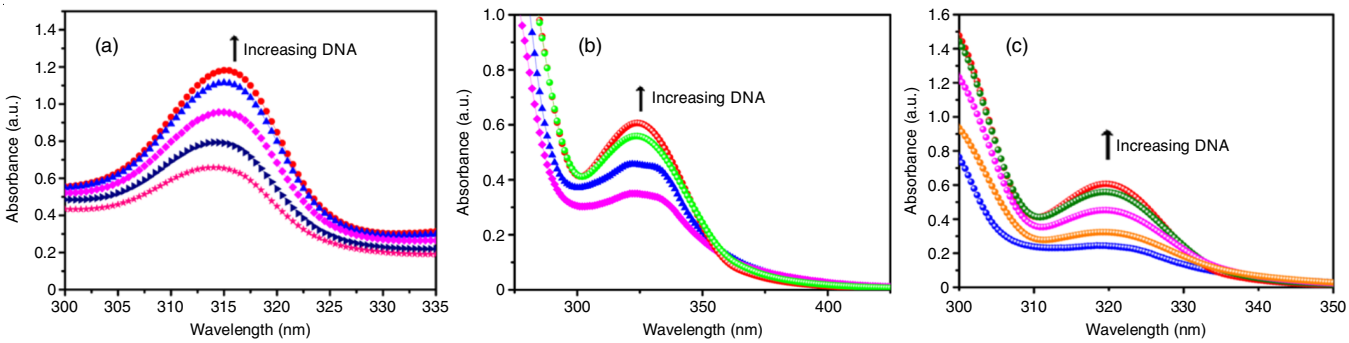

Fig. 5. Electronic absorption spectra of [CuL_2(phen)] (a); [CoL_2(phen)] (b) and [NiL_2(phen)] (c) in 5 mM Tris-HCl/50 mM NaCl buffer (pH = 7.2 at 298 K) in the presence of increasing amount of CT-DNA

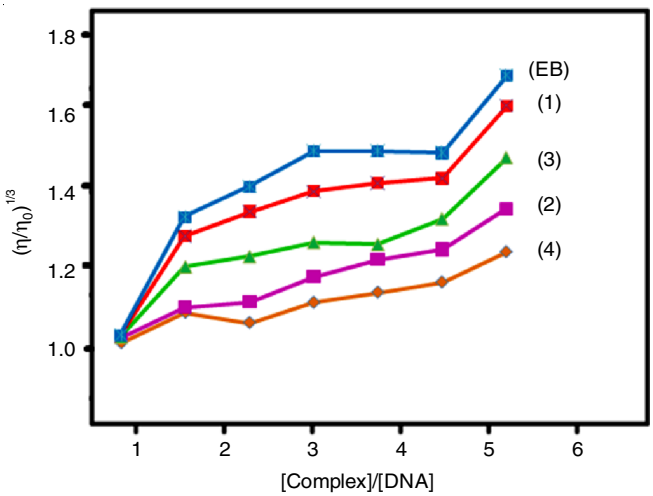

Fig. 6. Effects of increasing amount of classical intercalator [EB] and [ML_2(phen)] complexes on the relative viscosity of CT-DNA in 5 mmol Tris-HCl/50 mmol NaCl buffer at room temperature, where (1) Cu(II), (2) Co(II), (3) Ni(II) and (4) Zn(II) complexes

TABLE-3
MINIMUM INHIBITORY CONCENTRATION OF THE SYNTHESIZED COMPOUNDS AGAINST THE GROWTH OF BACTERIA (μM)

Compound	MIC values (× 10^4 μM) SEM = ± 1.5				
	S. aureus	*B. subtilis*	*E. coli*	*K. pneumoniae*	*S. typhi*
Ligand	14.6	13.5	14.3	12.8	13.2
Cu(II)	6.1	6.9	6.3	6.9	7.0
Co(II)	6.6	6.8	6.5	7.1	8.2
Ni(II)	6.3	6.7	6.2	7.1	7.2
Zn(II)	7.0	8.1	8.7	8.3	8.5
Ampicillin	5.8	6.6	6.8	7.2	7.5

TABLE-4
MINIMUM INHIBITORY CONCENTRATION OF THE SYNTHESIZED COMPOUNDS AGAINST THE GROWTH OF FUNGI (μM)

Compound	MIC values (× 10^4 μM) SEM = ± 1.3				
	A. niger	*F. solani*	*C. lunata*	*R. bataticola*	*C. albicans*
Ligand	20.2	15.5	18.6	21.5	22.2
Cu(II)	9.8	9.4	9.9	9.2	9.1
Co(II)	10.6	10.8	10.4	10.2	11.5
Ni(II)	9.8	9.2	9.5	9.6	10.5
Zn(II)	10.2	10.7	10.4	10.6	10.2
Nystatin	6.8	6.2	6.5	7.2	7.0

which possess MIC value of 5.8-7.5 × 10^4 μM. These MIC values are comparatively equal to standard drug ampicillin. In antifungal studies, Cu(II) complex has 9.1-9.9 × 10^4 μM and standard drug nystatin, which has MIC scores ranges from 6.2 to 7.2 × 10^4 μM. Therefore, mixed ligand metal(II) complexes have somewhat low activity than standard drug nystatin.

The screening ability of the synthesized mixed ligands metal(II) complexes depend on few factors, such as chelating effect of ligand, nature of donor cells, metal ions, counter ions that neutralizing the total charge and geometry of the complex. Metal complexes have higher antipathogenic ability than ligand and it could be explained by chelation concept. Upon chelation, the polarization of the metal ion decreases, due to the partial distribution of its positive charge with donor groups and potential π-electron delocalization of aromatic rings with phenyl rings [47]. It enhances the lipophilicity and supports to penetrate the cell membrane by blocking the metal targeted sites inside the enzymes of the microbial cell. It distracts the respiratory process of the cells and thereby inhibiting the synthesis of proteins, which prevents further growth of the organisms.

Anticancer studies: Anticancer therapy can be defined as the utilization of antitumor medications to hinder or prevent the proliferation of malignant tissues [48]. The previous studies on DNA synergy and gap have provided motivation to investigate the antiproliferative effect of the drugs against three different cell lines *viz*. human breast cancer cell line (MCF-7), human liver cancer cell (Hep G2) and non-cancerous cell line from human breast milk (HBL-100) by MTT assay and cisplatin act as a standard. The experiment depends upon the living cells are transformed into yellow MTT except for the non-living cells, which tend to display the blue formazan products. Hence, the metabolic action of the cells is assessed by the ability to split the tetrazolium rings of yellow MTT, which create the blue formazan product. The action of the cell activity was expressed as IC_{50} values.

All of the synthesized metal chelates demonstrate favourable anticancer properties, evidenced by their low IC_{50} values. Furthermore, the cytotoxic effects of the metal(II) complexes are observed to decrease as the concentration of metal complexes increases, indicating a dosage and time-dependent relationship. All the mixed ligand metal(II) complexes exhibit an excellent function against cancer cell lines due to chelation. Upon chelation, the metal centre has a positive charge, which augments the acidic behaviour of the entire compound that

accepts protons [49]. Among the synthesized mixed ligand metal(II) complexes, Cu(II) complex has IC_{50} values from 15-16 μM and anticancer activity is somewhat lower than standard cis-platin (IC_{50} values 10-11 μM). The anticarcinogenic action of the compounds could be related to the extended planar structure triggered by π→π* transition resulting in the chelation of metal with the free ligand. Further, it minimizes their polarization ability through the charge equilibration, which induces the dispersion of the compounds *via* the lipid membrane based on Tweedy's chelation theory [50]. Among the synthesized compounds, copper(II) complex exhibits excellent anticancer ability due to the size, ionic radius, lipophilicity behaviour of metal ion, hydrophobic character of heterocyclic ligand 1,10-phenanthroline which is important to boost the performance in this effect. The cytotoxic activity of the synthesized compounds is shown in Fig. 7 and enlisted in Table-5.

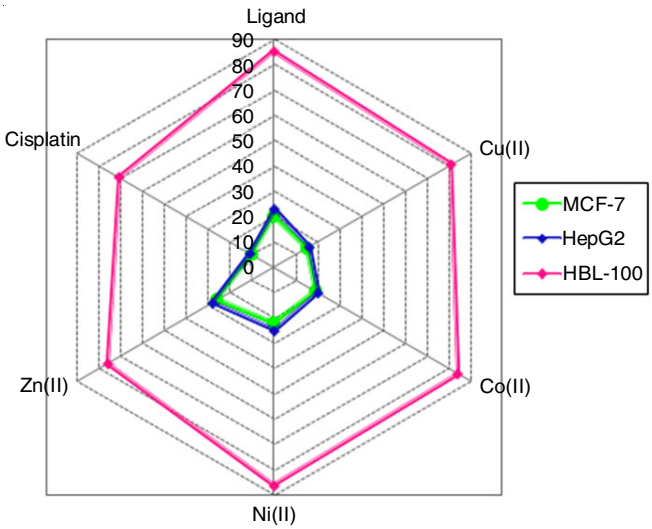

Fig. 7. Cytotoxic study of the synthesized compounds with breast adenocarcinoma (MCF-7), human liver cancer (Hep G2) and non-cancerous cell lines such as HBL-100 by MTT assay

TABLE-5
CYTOTOXIC ACTIVITY OF THE SYNTHESIZED COMPOUNDS AGAINST VARIOUS HUMAN CELL LINES

Compound	IC_{50} values (μM)		
	MCF-7	HepG 2	HBL-100
Ligand	20 ± 0.3	23 ± 0.2	85 ± 0.3
Cu(II)	15 ± 0.4	16 ± 0.2	81 ± 0.5
Co(II)	19 ± 0.5	20 ± 0.2	84 ± 0.8
Ni(II)	22 ± 0.2	25 ± 0.5	86 ± 0.3
Zn(II)	26 ± 0.2	28 ± 0.2	76 ± 0.3
Cisplatin	10 ± 0.1	11 ± 0.6	71 ± 0.4

Radical scavenging studies: The experiment was carried out with DPPH assay and vitamin C as standard. The outcomes implied that the mixed ligand metal(II) complexes have greater scavenging talent because of chelation [51]. The inhibitory activity data of the synthesized compounds is shown in Table-6. These data indicated that all the metal(II) complexes exhibit 50-75% scavenging efficiency levels, the Zn(II) complex has higher efficiency of 74.77% among all other synthesized metal (II) complexes. In comparison to the standard vitamin C, the synthesized metal(II) complexes have a scavenging ability ranging from 69% to 84%, however, their efficiency is slightly lower.

TABLE-6
ANTIOXIDANT ACTIVITY DATA (%) OF THE SYNTHESIZED COMPOUNDS

Compound	Concentration (μg/mL)			
	10	20	30	40
Ligand	12.40	15.73	22.41	28.37
Cu(II)	61.26	64.23	68.32	72.81
Co(II)	55.50	68.22	67.91	72.79
Ni(II)	50.30	60.25	65.71	70.20
Zn(II)	60.30	65.44	70.33	74.77
Vitamin C	69.82	78.47	82.45	84.23

Docking simulation: Docking simulation is a structure-based drug design and verifies the binding affinity of the small compound to the specific targeted binding site [52]. It is an interactive molecular graphics program for knowing drug and DNA interactions. Docking is performed with epidermal growth factor receptor (EGFR) protein using Autodock Vina software. EGFR is a protein, which is present on the outer cover of body tissues that break down cells, when the epidermal growth factor interacts to it. This is an inhibitor to slow down or inhibit the cell development. Some type of cancers can get mutations in their EGFR that can cause uncontrolled cell fractionation *via* continuous or abnormal activation.

Autodock Vina software was used to analyze the interaction. The relative binding energy calculated for the Schiff base ligand was found to be -235 kJ mol^{-1}, whereas for the mixed ligand metal(II) complexes were found to be -333, -330, -324 and -313 kJ mol^{-1} for Cu(II), Co(II), Ni(II) and Zn(II) complexes, respectively. The compounds which have high negative binding energy signifies that greater binding affinity [53]. It is clear from the results obtained that the presence of the metal ion in the molecule reduces the binding energies, but increases the binding affinity. As a result, it exhibits a high biological potential of the metal(II) complexes. In contact with FGFR, Schiff base ligand stabilized the H-bond between hydrogen from oxygen and hydroxyl group from histidine group. The Cu(II) complex formed two hydrogen bonds with valine and glycine, respectively, with 3.7 Å and 4.6 Å bond distances, whereas Co(II) complex formed two hydrogen bonds with lysin and valine with bond distances 3.7 Å and 3.5 Å. Nickel(II) complex formed two hydrogen bonds with leucine and valine with bond distances 4.2 Å and 4.5 Å, while zinc(II) complex also formed two hydrogen bonds with alanine and arginine with bond distance 5.0 Å and 5.8 Å. Thus, based on the outputs, copper compound shows greater binding affinity due to the highest negative value. The binding model of the synthesized compounds with protein are shown in in Fig. 8.

Docking studies was also performed for the synthesized compounds against 1B-DNA. The stacking energy of the synthesized compounds with 1B-DNA found to be around -250 to -380 kJ mol^{-1}. The presence of carbonyl oxygen with high electronegativity in the compounds disrupts the hydrogen bonds between the nucleotide base pairs. The results of the molecular docking study show that the compounds bind effici-

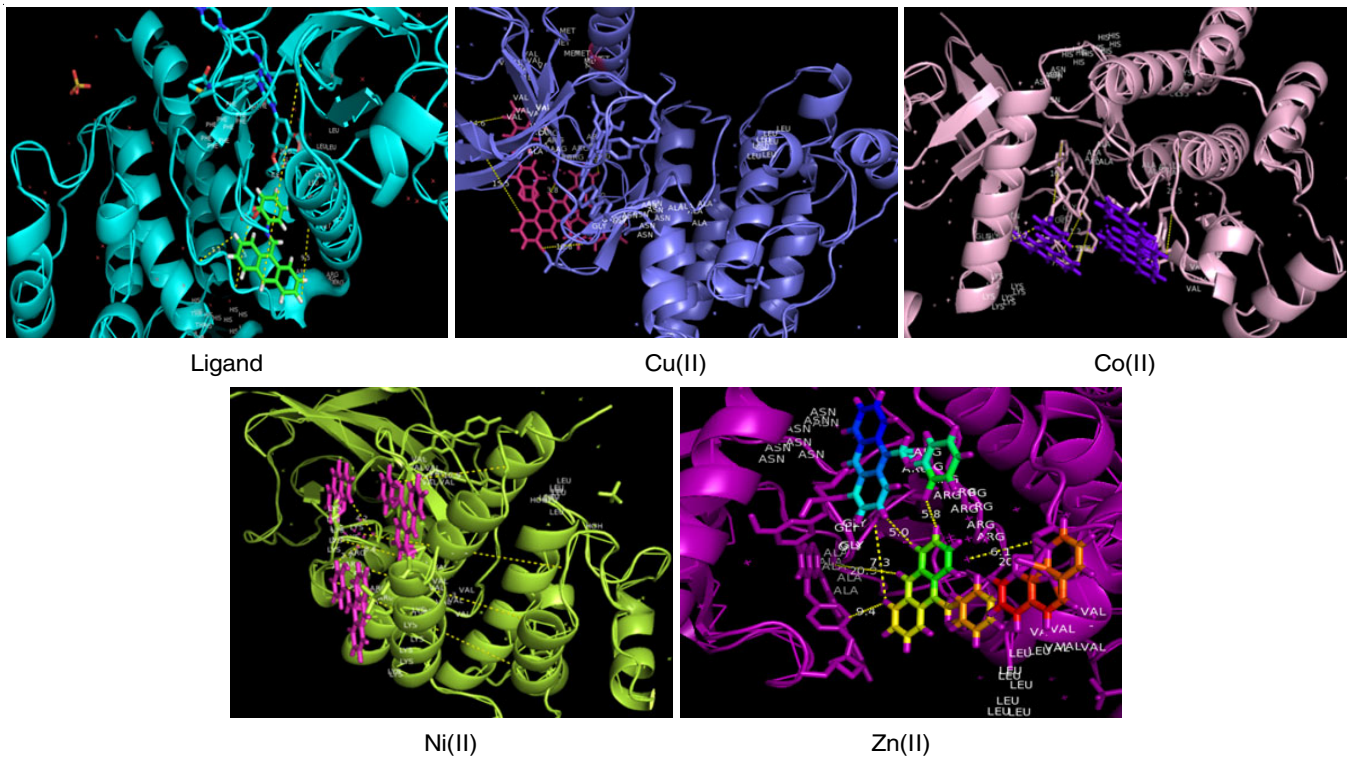

Fig. 8. Binding model of synthesized compounds with EGFR protein

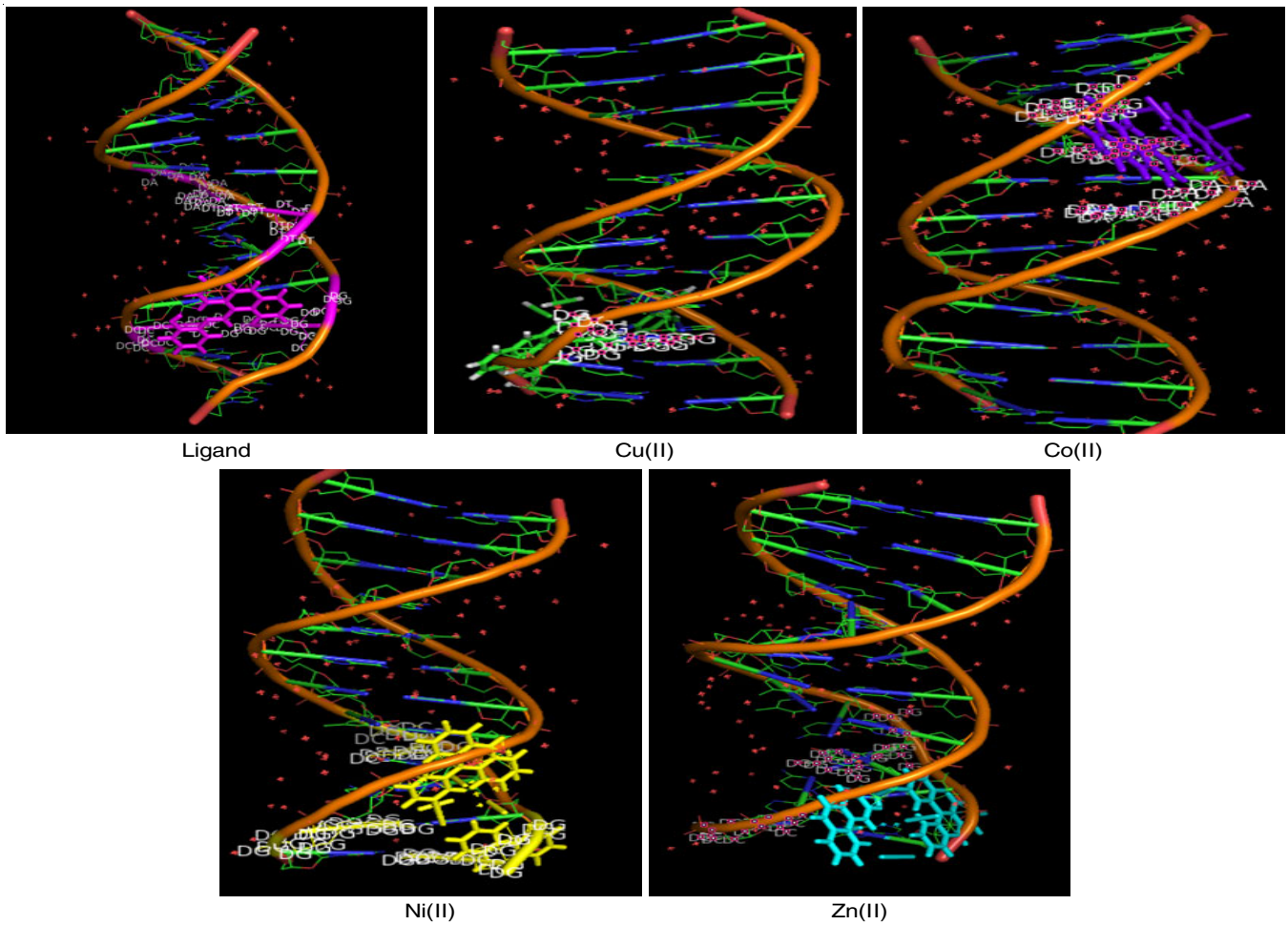

Fig. 9. Binding model of synthesized compound with 1B-DNA receptor

ently to the DNA receptor from their binding energy values. Among the compounds, Cu(II) complex showed a high binding affinity (-380 kJ mol^{-1}) to the DNA molecule and contributed to most of the hydrogen bonds to the guanine. Therefore, the Cu(II) complex has a better chance of disrupting and mutating DNA molecules. These molecules stand as an opportunity to become drug molecules for the treatment of cancer and DNA-targeted drug delivery systems. The binding model of the synthesized compounds with DNA is shown in Fig. 9. The results from the simulation studies agree well with the results from the analyses.

Conclusion

A novel heterocyclic Schiff base and mixed ligand metal(II) complexes with improved pharmacological properties have been synthesized and characterized. The mode of interaction with DNA was affirmed by the docking simulations, where the synthesized compounds were docked with EGFR protein and 1B-DNA through intercalation. The screening study against microbes was analyzed and the outputs evinced that complexes were excellent anti-pathogenic screeners rather than ligand. The proliferation resistance against cancer cells and free radical scavenger studies of the synthesized compounds indicated that the presence of heterocyclic ligand is an important factor for boosting the anticancer potential and radical scavenger skill. From the biological results, the comparative activity of the $[CuL_2(phen)]$ complex in relation to other complexes is evident, despite the fact that all molecules exhibit biological efficacy. Finally, it establishes a strong foundation for the metal-derived antitumor medicines on the theory of selected target, which it believes will be crucial in the future when choosing cancer cells and making therapeutic drugs.

ACKNOWLEDGEMENTS

One of the authors, SSAF, gratefully acknowledges the Kalasalingam Academy of Research and Education for offering research fellowship and necessary facilities.

CONFLICT OF INTEREST

The authors declare that there is no conflict of interests regarding the publication of this article.

REFERENCES

1. T. Ashraf, B. Ali, H. Qayyum, M.S. Haroone and G. Shabbir, *Inorg. Chem. Commun.*, **150**, 110449 (2023); https://doi.org/10.1016/j.inoche.2023.110449
2. A.M. Florea and D. Busselberg, *Cancers*, **3**, 1351 (2011); https://doi.org/10.3390/cancers3011351
3. M.A. Fuertes, C. Alonso and J.M. Perez, *Chem. Rev.*, **103**, 645 (2003); https://doi.org/10.1021/cr020010d
4. N. Shahid, N. Sami, M. Shakir and M. Aatif, *J. Saudi Chem. Soc.*, **23**, 315 (2019); https://doi.org/10.1016/j.jscs.2018.08.004
5. R. Anjum, D. Palanimuthu, D.S. Kalinowski, W. Lewis, K.C. Park, Z. Kovacevic, I.U. Khan and D.R. Richardson, *Inorg. Chem.*, **58**, 13709 (2019); https://doi.org/10.1021/acs.inorgchem.9b01281
6. C. Santini, M. Pellei, V. Gandin, M. Porchia, F. Tisato and C. Marzano, *Chem. Rev.*, **114**, 815 (2014); https://doi.org/10.1021/cr400135x
7. S.B. Chanu, S. Banerjee and M. Roy, *Eur. J. Med. Chem.*, **125**, 816 (2017); https://doi.org/10.1016/j.ejmech.2016.09.090
8. L. Ruiz-Azuara and M.E. Bravo-Gomez, *Curr. Med. Chem.*, **17**, 3606 (2010); https://doi.org/10.2174/092986710793213751
9. R. Lugano, M. Ramachandran and A. Dimberg, *Cell Mol. Life Sci.*, **77**, 1745 (2020); https://doi.org/10.1007/s00018-019-03351-7
10. M.M. Eatock, A. Schatzlein and S.B. Kaye, *Cancer Treat. Rev.*, **26**, 191 (2000); https://doi.org/10.1053/ctrv.1999.0158
11. H. Xie and Y.J. Kang, *Curr. Med. Chem.*, **16**, 1304 (2009); https://doi.org/10.2174/092986709787846622
12. A. Gupte and R.J. Mumper, *Cancer Treat. Rev.*, **35**, 32 (2009); https://doi.org/10.1016/j.ctrv.2008.07.004
13. F. Tisato, C. Marzano, M. Porchia, M. Pellei and C. Santini, *Med. Res. Rev.*, **30**, 708 (2010); https://doi.org/10.1002/med.20174
14. K.L. Haas and K.J. Franz, *Chem. Rev.*, **109**, 4921 (2009); https://doi.org/10.1021/cr900134a
15. M. Chikira, C.H. Ng and M. Palaniandavar, *Int. J. Mol. Sci.*, **16**, 22754 (2015); https://doi.org/10.3390/ijms160922754
16. S.K. Singh, S. Joshi, A.R. Singh, J.K. Saxena and D.S. Pandey, *Inorg. Chem.*, **46**, 10869 (2007); https://doi.org/10.1021/ic700885m
17. Y. Li, G. Zhang and M. Tao, *J. Photochem. Photobiol.* B, **138**, 109 (2014); https://doi.org/10.1016/j.jphotobiol.2014.05.011
18. A.K. Sadana, Y. Mirza, K.R. Aneja and O. Prakash, *Eur. J. Med. Chem.*, **38**, 533 (2003); https://doi.org/10.1016/s0223-5234(03)00061-8
19. M. Chauhan, K. Banerjee and F. Arjmand, *Inorg. Chem.*, **46**, 3072 (2007); https://doi.org/10.1021/ic061753a
20. N. Udilova, A.V. Kozlov, W. Bieberschulte, K. Frei, K. Ehrenberger and H. Nohl, *Biochem. Pharm.*, **65**, 59 (2003); https://doi.org/10.1016/s0006-2952(02)01452-1
21. M. Sonmez, M. Celebi and I. Berber, *Eur. J. Med. Chem.*, **45**, 1935 (2010); https://doi.org/10.1016/j.ejmech.2010.06.016
22. E. Oruc, S. Rollas, F. Kandemirili, N. Shvets and A.S. Dimoglo, *J. Med. Chem.*, **47**, 6760 (2004); https://doi.org/10.1021/jm0495632
23. A. Lagunin, D. Filimonov and V. Poroikov, *Curr. Pharm. Des.*, **16**, 1703 (2010); https://doi.org/10.2174/138161210791164063
24. M.D. Segall, A.P. Beresford, J.M.R. Gola, D. Hawksley and M.H. Tarbit, *Expert Opin. Drug Metab. Toxicol.*, **2**, 325 (2006); https://doi.org/10.1517/17425255.2.2.325
25 F. Liu and B. Fang, *Chinese J. Biotechnol.*, **23**, 133 (2007); https://doi.org/10.1016/S1872-2075(07)60012-0
26. H. Chen, J.A. Parkinson, R.E. Morris and P.J. Sadler, *J. Am. Chem. Soc.*, **125**, 173 (2003); https://doi.org/10.1021/ja027719m
27. R.S. Kumar and S. Arunachalam, *Polyhedron*, **26**, 3255 (2007); https://doi.org/10.1016/j.poly.2007.03.001
28. C. Justin Dhanaraj and J. Johnson, *Spectrochim. Acta A Mol. Biomol. Spectrosc.*, **118**, 624 (2014); https://doi.org/10.1016/j.saa.2013.09.007
29. A.R. Silva, M.M.A. Freitas, C. Freire, B. de Castro, J.L. Figueiredo, *Langmuir*, **18**, 8017 (2002).
30. D.X. West, A.A. Nassar, F.A. El-Saied, M.I. Ayad, D.X. West, A.A. Nassar, F.A. El-Saied, *Transition Met. Chem.*, **23**, 321 (1998); https://doi.org/10.1023/A:1006957325074
31. K.R. Wilson, D.J. Cannon-Smith, O.C. Birdsong, S.J. Archibald, B.P. Burke and T.J. Hubin, *Polyhedron*, **114**, 118 (2016); https://doi.org/10.1016/j.poly.2015.11.014
32. G.B. Bagihalli, P.G. Avaji, S.A. Patil and P.S. Badami, *Eur. J. Med. Chem.*, **43**, 2639 (2008); https://doi.org/10.1016/j.ejmech.2008.02.013
33. M. Manimohan, S. Pugalmani, K. Ravichandran and M.A. Sithique, *RSC Adv.*, **10**, 18259 (2020); https://doi.org/10.1039/D0RA01724H

34. G. Garcia-Friaza, A. Fernandez-Betello, J.M. Perez, M.J. Prieto and V. Moreno, *J. Inorg. Biochem*, **100**, 1368 (2006); https://doi.org/10.1016/j.jinorgbio.2006.03.011
35. K. Dyrek and M. Che, *Chem. Rev.*, **97**, 305 (1997); https://doi.org/10.1021/cr950259d
36. K. Satyanarayana and M.N.A. Rao, *Eur. J. Med. Chem.*, **30**, 641 (1995); https://doi.org/10.1016/0223-5234(96)88280-8
37. N. Raman, S.F.S. Ali and D.J. Raja, *J. Serbian Chem. Soc.*, **73**, 1063 (2008); https://doi.org/10.2298/JSC0811063R
38. R.J. Dudley and B.J. Hathaway, *J. Chem. Soc. A*, **0**, 2794 (1970); https://doi.org/10.1039/J19700002794
39. P. Pakravan and S. Masoudian, *Iran. J. Pharm. Res.*, **14**, 111 (2015).
40. E.T. Knittl, A.A. Abou-Hussein and W. Linert, *Monatsh. Chem.*, **149**, 431 (2018); https://doi.org/10.1007/s00706-017-2075-9
41. R. Antony, S. Theodore David Manickam, K. Karuppasamy, P. Kollu, P.V. Chandrasekar and S. Balakumar, *RSC Adv.*, **4**, 42816 (2014); https://doi.org/10.1039/C4RA08303B
42. Z.H. Chohan, M. Arif and M. Sarfraz, *Appl. Organomet. Chem.*, **21**, 294 (2007); https://doi.org/10.1002/aoc.1200
43. B.J. Pages, D.L. Ang, E.P. Wright and J.R. Aldrich-Wright, *Dalton Trans.*, **44**, 3505 (2015); https://doi.org/10.1039/C4DT02700K
44. V. Rajendiran, M. Murali, E. Suresh, S. Sinha, K. Somasundaram, M. Palaniandavar, *Dalton Trans.*, 148 (2008); https://doi.org/10.1039/B710578A
45. S.A. Tysoe, R.J. Morgan, A.D. Baker and T.C. Strekas, *J. Phys. Chem.*, **97**, 1707 (1993); https://doi.org/10.1021/j100110a038
46. Clinical and Laboratory Standards Institute, Performance Standards for Antimicrobial Susceptibility Testing, Clinical and Laboratory Standards Institute (CLSI), USA, edn. 31, (2021).
47. Z.C. Liu, B.D. Wang, B. Li, Q. Wang, Z.-Y. Yang, T.-R. Li and Y. Li, *Eur. J. Med. Chem.*, **45**, 5353 (2010); https://doi.org/10.1016/j.ejmech.2010.08.060
48. H.H. Harris, A. Levina, C.T. Dillon, I. Mulyani, B. Lai, Z. Cai and P.A. Lay, *J. Biol. Inorg. Chem.*, **10**, 105 (2005); https://doi.org/10.1007/s00775-004-0617-1
49. S. Satyanarayana, J.C. Dabrowiak and J.B. Chaires, *Biochemistry*, **32**, 2573 (1993); https://doi.org/10.1021/bi00061a015
50. A. Tarushi, E. Polatoglou, J. Kljun, I. Turel, G. Psomas and D.P. Kessissoglou, *Dalton Trans.*, **40**, 9461 (2011); https://doi.org/10.1039/c1dt10870k
51. A.R. Silva, M.M.A. Freitas, C. Freire, B. de Castro and J.L. Figueiredo, *Langmuir*, **18**, 8017 (2002); https://doi.org/10.1021/la025833c
52. M. Shakir, S. Hanif, M.A. Sherwani, O. Mohammad and S.I. Al-Resayes, *J. Mol. Struct.*, **1092**, 143 (2015); https://doi.org/10.1016/j.molstruc.2015.03.012
53. M. Vasconcellos-Dias, C.D. Nunes, P.D. Vaz, P. Ferreira and M.J. Calhorda, *Eur. J. Inorg. Chem.*, **18**, 2917 (2007); https://doi.org/10.1002/ejic.200700091